Micro H-Darrieus wind turbines: CFD modeling and experimental validation

Cite as: AIP Conference Proceedings **2191**, 020109 (2019); https://doi.org/10.1063/1.5138842
Published Online: 17 December 2019

Stefano Mauro, Sebastian Brusca, Rosario Lanzafame, and Michele Messina

Micro H-Darrieus Wind Turbines: CFD Modeling And Experimental Validation

Stefano Mauro[1, a)], Sebastian Brusca[2, b)], Rosario Lanzafame[1, c)], Michele Messina[1, d)]

[1] *Department of Civil Engineering and Architecture, University of Catania, Via Santa Sofia 64, 95123 Catania, Italy*
[2] *Department of Engineering, University of Messina, Contrada Di Dio, 98166 Messina, Italy*

[a)]Corresponding author: mstefano@diim.unict.it
[b)]sbrusca@unime.it
[c)]rosario.lanzafame@unict.it
[d)]mmessina@dii.unict.it

Abstract. The scientific interest toward micro wind turbine power generation is growing thanks to the fact that these systems appear to be very suitable for small stand-alone devices such as controllers, actuators, sensors, small lightning systems which cannot be easily powered through electricity grids. Furthermore, micro wind turbines are widely used for wind tunnel testing as the wind tunnel dimensions are usually quite limited. The present paper deals with the CFD modeling of a micro H-Darrieus wind turbine, designed and tested in the subsonic wind tunnel, owned by the University of Catania. Such small rotors are usually very difficult to simulate accurately due to the very low Reynolds number effects and the strong unsteadiness related to their operation. Through the use of an accurate unsteady Delayed Detached Eddy Simulation approach for turbulence modeling, the authors demonstrated the possibility to obtain reliable CFD 2D model of such micro rotors. The modeling methodology was developed by means of an accurate grid and time step sensitivity study and by comparing different approaches for turbulence closure. The model was validated using data obtained from experiments carried out in the wind tunnel, which showed a rather satisfactory predictive capability of the model. Therefore, the proposed numerical model allowed for a better comprehension of the fluid dynamic behavior of such micro rotors. Furthermore, the model will be used for trying to optimize micro H-Darrieus turbines which usually show poor efficiency compared to micro horizontal axis wind turbines.

INTRODUCTION

Miniature and micro wind turbines have gained great attention for powering low-power devices such as wireless sensors, actuators, controllers and small lightning systems in all those conditions in which it is impossible to supply the devices through the electrical network. Usually, these devices are powered by means of chemical batteries which however must be periodically replaced therefore representing a challenge for a reliable power supply. For this reason small-size energy harvesters are of utmost importance in order to obtain reliable self-powered systems. Solar panels, hydrogen fuel cell, thermoelectric converters are some of the possibilities but they are expensive and not always usable. Thus, small-scale wind turbines represent an attractive solutions for the electricity generation in such small-size energy harvesters.

Previous studies about miniature wind turbines mainly focused on Horizontal Axis Wind Turbine (HAWT) due to the fact that these turbines had acceptable efficiency despite the small scale. Xu et al [1] developed an experimental test and a numerical predictive model on a miniature HAWT with a diameter of 15 cm. They obtained a maximum efficiency of approximately 27%. Kishore et al. [2 - 3] designed and characterized a small-scale portable wind turbine of about 40 cm which showed very low cut-in velocity and a maximum efficiency of 30% with a rated power of 1.4 W. Zakaria et al. [4] performed an experimental investigation of a centimeter-scale wind turbine. They showed the strong effect of the very low Reynolds number on the rotor performance as they obtained

74th ATI National Congress
AIP Conf. Proc. 2191, 020109-1–020109-10; https://doi.org/10.1063/1.5138842
Published by AIP Publishing. 978-0-7354-1938-4/$30.00

an efficiency of only 3-4%. An interesting application of miniature HAWT was proposed again by Xu et al. [5]. Here the authors developed a physical-based model for the prediction of the optimal load resistance and the experimental characterization of the micro turbine. The efficiency was found to be lower than 10%.

Another important use of micro wind turbine is the one for wind tunnel experiments. Indeed, the wind tunnel dimensions are usually limited and only small rotors can be tested. Bastankhah et al. [6] designed and analyzed a miniature wind turbine with a rotor diameter of 15 cm. They demonstrated that an accurate fluid dynamic design for specific low Reynolds number was of utmost importance for reaching high efficiency. In this case they obtained a maximum C_p of approximately 40%. The authors of the present paper presented a numerical and experimental study regarding a three bladed micro HAWT for wind tunnel applications [7]. An efficiency of about 30% was found. As far as VAWT was concerned, Mutlu et al. [8] evaluated the performance of in-pipe VAWT for turbo solenoid valve system, finding interesting results.

All these studies demonstrate the scientific interest toward micro wind rotors and highlight the fact that such small rotors need for a very fine fluid dynamic design in order to obtain high efficiency. This is due to the fact that the very low Reynolds numbers drastically reduce the airfoil performances and the small dimensions emphasize the unsteadiness and the 3D losses like tip effects.

In the present work, the authors developed a 2D CFD model of a H-Darrieus VAWT with a diameter of 20 cm. The CFD model was validated by means of wind tunnel experiments carried out in the subsonic wind tunnel owned by the University of Catania. The widely known difficulties of the CFD in the simulation of very small VAWT made the study even more interesting. This involves that most of the CFD modeling procedures proposed in the literature for largest rotors might not be suitable for micro VAWTs. The experimental H-Darrieus rotor had 4 NACA 0012 blades and it was designed and constructed with a 3D printer. Further details about the experimental set up are presented in the next section. In order to develop an accurate and reliable CFD model of such micro rotor, a thorough sensitivity study was carried out. The study analyzed the grid sensitivity, the temporal discretization sensitivity and three turbulence models in such a way to obtain the best compromise between numerical accuracy and computation time. The turbulence model evaluated were: the Reynolds Averaged Navier Stokes (RANS) fully turbulent SST k-ω model with low Re correction, the RANS transition SST model by Menter and an advanced Delayed Detached Eddy Simulation model (DDES) which used the transition SST model by Menter for the RANS region and the Large Eddie Simulation (LES) for the outer region. Furthermore, the results were compared to that obtained through the use of a double multiple stream-tube 1D model (DMSTM) using the commercial software Qblade.

NUMERICAL MODEL AND EXPERIMENTAL SETUP

The CFD 2D numerical model presented in this paper was based on a wide literature background which however deals mainly with larger rotors. These rotors operated in more stable conditions and higher Reynolds numbers therefore their modeling, in general, led to accurate and reliable results. The present study instead focused on the development of a numerical procedure dedicated specifically to very micro H-Darrieus rotor in which highly unstable conditions must be simulated. However, numerous useful suggestions was found in the literature as reported hereinafter. Balduzzi et al. made interesting studies about the critical issues in the CFD simulations of H-Darrieus rotors [9], the effectiveness of 2D CFD simulations for H-Darrieus rotors [10] and an assessment of mesh and time-step requirements in CFD 2D simulations of H-Darrieus wind turbines [11]. These works provided important guidelines for the development of accurate and reliable CFD 2D models of VAWTs, therefore allowing for a reduction of the time required for the spatial and temporal independency study. The authors of the present paper, previously developed a 2D CFD modeling strategy for moderately large H-Darrieus [12] demonstrating the good accuracy of the transition turbulence model by Menter in cases in which the laminar to turbulent boundary layer transition played an essential role.

The last works showed that, beyond the domain size, there was no strong agreement about the adequate spatial and temporal discretization as well. However, some guidelines can be obtained. For example, a y^+ less than one near the blades was universally considered an essential constraint. A time step size, such that the azimuthal increment was at least below 0.5 degree, was equally important. When boundary layer transition phenomena are detected, a transition turbulence model strongly increased the accuracy of the CFD models [12, 13]. Nevertheless, many authors evidenced the superior accuracy of advanced turbulence modeling like hybrid RANS-LES formulations, above all when the rotor are subjected to highly unstable condition. Strong dynamic stall, high blade-wake interaction and vortices related to the flow separation were certainly more accurately predicted through the use of hybrid RANS-

LES models like DES and Delayed DES. Indeed, in a recent paper, Lei et al. [14] demonstrated that improved DDES simulation was able to capture real flow characteristics, like those generated by vortices related to dynamic stall phenomena, that were not predicted by the SST k- ω model. Thè et al. [15] in their thorough review showed that DDES simulations represented the best compromise between very high accuracy and computation requirements for the simulation of the unstable conditions related to the VAWTs. Simão Ferreira et al. [16 - 17] performed a complete numerical-experimental comparison between RANS, DES and LES turbulence models using accurate Particle Image Velocimetry (PIV) data. They also suggested precise prescriptions for the spatial and temporal discretization related to the specific turbulence modeling. Therefore the DDES turbulence model coupled to the transition turbulence model by Menter [18 - 20], recently implemented in the ANSYS Fluent solver, appeared to be very suitable for the scope of the present work. In order to confirm this assumption and to maximize the accuracy of the numerical prediction, a comparison between the fully turbulent SST k-ω model, the SST transition model and the DDES, coupled with the SST transition model, was carried out hereinafter.

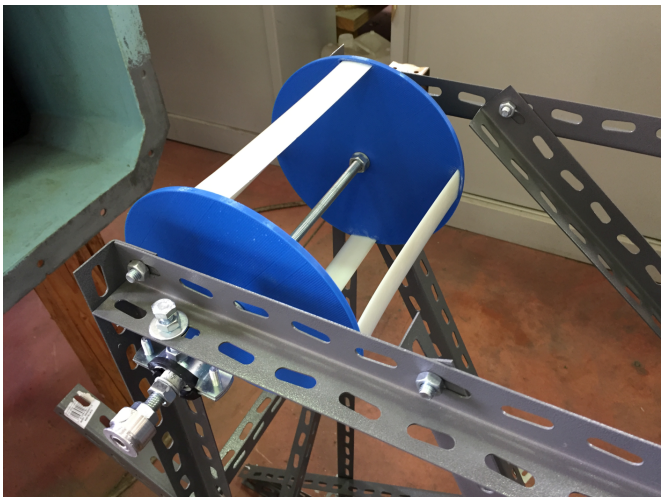

FIGURE 1. Experimental rotor

TABLE 1. Experimental rotor features

Geometrical and experimental characteristics	
Diameter [m]	0.2
Height [m]	0.2
Cord [m]	0.03
Number of blades	4
Solidity	0.19
Blade airfoil	NACA 0012
Pitch [deg]	0
Shaft diameter [m]	0.01
Maximum Re	~ 50,000
Bearings	2 Needle Roller Bearings
Flow speed range [m/s]	11 - 21
Rotational speed range [r/min]	27 - 580
Tip speed ratio range	0.025 - 0.29

The experimental turbine used in this work was a four bladed H-Darrieus rotor with square shape, therefore having a ratio between height (H) and diameter (D) equal to one. Two endplates were used for the reduction of the tip losses in such a way to make the experimental results consistent with the 2D simulations. The blades were built in a resin 3D printer which allowed for very high accuracy of the details and a very fine surface roughness. The endplates were instead built in a 3D printer with PLA material. For the shaft a steel threaded bar was used. The geometrical and experimental rotor features are reported in Table 1 while if Fig. 1 an image of the rotor within the experimental setup is shown. As far as the experimental setup is concerned, the subsonic wind tunnel owned by the

University of Catania was used. Details about the wind tunnel are reported in [7, 21]. The flow speed was measured thorough the use of a Pitot probe. The rotational speed was measured by means of a digital laser tachometer. The torque was evaluated by using a specifically designed braking system, based on the principle of the belt brake. The instantaneous brake force was measured through a load cell and the torque was obtained. The rotor was suspended at the support structure through two needle roller bearings and the torque losses were experimentally evaluated as a function of the rotational speed. The flow and rotational speed range is reported in Table 1.

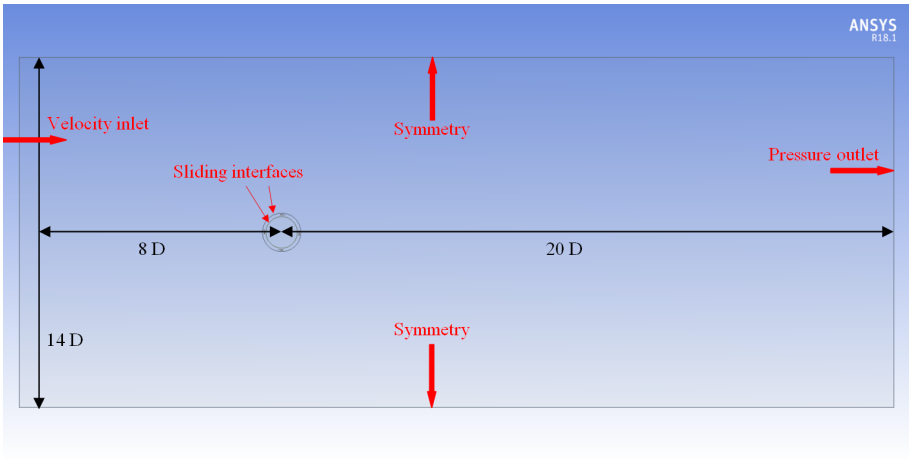

FIGURE 2. Computational domain dimensions and boundary conditions

The CFD 2D simulations were implemented for five specific operating conditions (different couples of flow speed and rotational speed equal to the experimental one, Table 4) in such a way to cover the entire range of tip speed ratio. Based on the wide literature analyzed, the first step in the development of the CFD 2D model was the definition of the suitable computational domain. Since there was no strong agreement about the adequate domain dimensions to have independent results, a specific study was made here. In this case the best compromise for the domain dimensions is shown in Figure 2. It was verified that much larger domains did not affect the solution. Moreover, the use of the symmetry condition for the lateral boundaries further reduced the possible influences of the domain dimensions on the flow-field. Concerning the boundary conditions, those used in the present work are shown in Figure 2 as well. For the simulation of the rotating zone the same technique as in [12] was implemented. The domain was divided into three sub-domains in order to implement the unsteady sliding mesh model (SMM) in a rotating ring which contained the four blades. The internal circle and the outer domain remained stationary. The external and internal circumferences of the ring were thus set as sliding interfaces (Figure 2).

The greatest efforts in this work were made in order to obtain an adequate level of spatial and temporal discretization in such a way to guarantee the best compromise between accuracy and computation time. Specifically, as the tip speed ratio was reduced the grid refinement must be increased in order to adequately capture the higher vorticity gradients related to the unstable operating condition [9 - 11]. Furthermore, the temporal discretization must be reduced accordingly to the grid refinement so as the Courant number remained below 10 thus providing the optimal error damping properties in implicit scheme solver.

Therefore, due to the highly unstable condition related to the very low operating tip speed ratios of the micro rotor (between 0.025 and 0.29 in Table 1), a specific spatial and temporal sensitivity study, for each of the three turbulence models, was carried out. Three meshing levels and three time steps were tested for each of the three turbulence models, leading to 9 sensitivity tests for each rotor operating condition. The tests were conducted for the maximum ($\lambda = 0.29$) and the minimum ($\lambda = 0.025$) tip speed ratio in order to find the best compromise for all the intermediate simulations. Regarding the computational grid, the specific meshing characteristics for the three refinement levels are reported in Table 2 and are named as Mesh 1, the coarsest one, Mesh 2, the first refinement level, and Mesh 3 the second refinement level or the finest one. The blade boundary layer was discretized using quadrangular elements, inflated from the blade walls. As widely known, the quadrangular elements are necessary for an adequate resolution of the boundary layer. The first layer height was fixed in such a way to guarantee a $y^+ < 1$for all the simulations as prescribed by the turbulence models [18 - 20]. For the stationary outer domain, a sizing function, which limited the maximum dimension of the elements, was used. In Fig. 3 some details of the Mesh 2 are showed. It is work to remark that Mesh 2 and Mesh 3 did satisfy the criterion proposed by Balduzzi et al. [10] about

the Grid Reduced Vorticity (GRV) as a quantitative parameter for a qualitative a priori evaluation of the spatial discretization accuracy. GRV is a vorticity normalized with respect to the local grid size and thus gives an estimate of the velocity variation within a single element. In the present paper it was verified that Mesh 2 and Mesh 3 had GRV < 1%, as recommended by [10] while Mesh 1 presented values slightly above. All the tested grids satisfied the LES filter constraint imposed by the DDES model which was to have cell dimension lower than 1/30 the cord length [22].

TABLE 2. Grid independence study meshing characteristics

Grid features	Mesh 1 (M1)	Mesh 2 (M2)	Mesh 3 (M3)
Number of elements	320,000	800,000	2,170,000
Nodes on airfoil	1,000	2,000	4,000
Rotating domain sizing	7.5 e^{-4} m	5 e^{-4} m	2.5 e^{-4} m
Inner circle sizing	7.5 e^{-4} m	5 e^{-4} m	2.5 e^{-4} m
Outer domain sizing	0.01 m	0.01 m	0.01 m
Global growth rate	1.2	1.1	1.05
Inflation layers	20	40	60
First layer height	1 e^{-6} m	1 e^{-6} m	1 e^{-6} m
Skewness max	0.77	0.72	0.79
Y^+ max	0.25	0.23	0.22

As far as the temporal discretization was concerned, the time step dimension was set in such a way to have a wide set of Courant numbers for testing. The Courant number was defined as:

$$\boldsymbol{Co = V \frac{\Delta t}{\Delta x}} \tag{1}$$

For VAWTs, V is the peripheral velocity of the airfoil, Δx is the average distance between nodes on airfoil and Δt is the time step. The Courant Number expresses the ratio between the temporal time step (Δt) and the time required by a fluid particle, moving with V velocity, to be convected throughout a cell of dimension Δx [10].

Being V the peripheral velocity, in order to obtain similar Courant numbers, the time step must be varied as the tip speed ratio changed. This meant to keep the same angular step as the rotational speed varied, due to the fact that in this work both the flow and the rotational speed changed. In Table 3 the Courant numbers, obtained for different combination of grids and time steps, are shown.

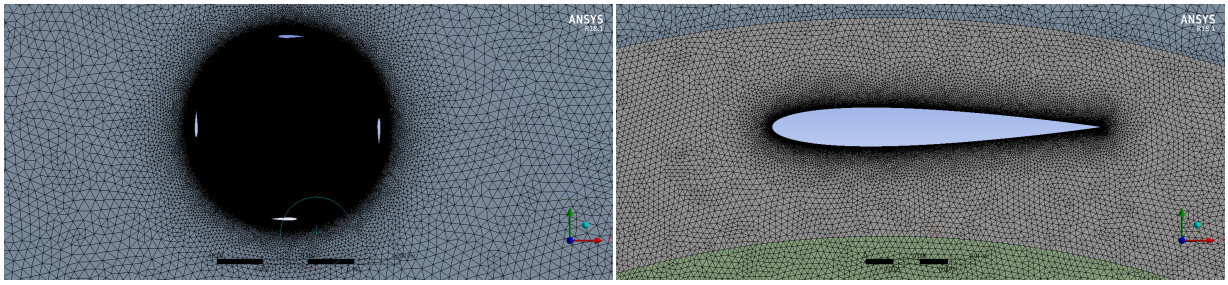

(a) (b)

FIGURE 3. Details of Mesh 2

The results of the sensitivity study are shown in Fig. 4. The charts present the trend of the average torque coefficient for the various combination of grids, angular steps and turbulence models. Specifically, the average torque coefficient is parameterized as a function of angular step and number of grid elements in each chart. Figures 4 (a) and (b) are related to the DDES model at maximum (a) and minimum (b) tip speed ratio respectively. Figures 4 (c) and (d) refer to the RANS SST transition model while Fig. 4 (e) and (f) regard the RANS SST k-ω model. Globally, the sensitivity analysis demonstrates that the grids M2 and M3 with angular steps Δθ = 0.035° and Δθ = 0.01° lead to results which are in very close proximity. For the DDES turbulence model, the percentage difference is approximately 1%. Therefore, mesh M2 with an angular step equal to Δθ = 0.035° was the best compromise for the minimization of the spatial and temporal discretization errors for all the simulated range of tip speed ratio. However,

it is worth evidencing that both the RANS turbulence models highly underestimate the average torque coefficient with respect to the DDES model. They even predict negative average torque coefficients at λ_{max}. This suggests that in highly unstable conditions, related to the micro VAWTs, the RANS turbulence models lead to wrong physical predictions of the flow-field. Instead, comparing the experimental and numerical results, the very high accuracy obtained with the DDES model will be demonstrated hereinafter.

TABLE 3. Courant numbers for the different grids and time steps at maximum and minimum λ

Δθ [deg]	Δt [s]	Δx [mm]			λ [-]
		0,03 (M1)	0,015 (M2)	0,0075 (M3)	
		Co [-]			
0,1	0,00003	6,07	12,15	24,29	
0,035	0,00001	2,02	4,05	8,10	0,29
0,01	0,000003	0,61	1,21	2,43	
0,1	0,00062	5,84	11,69	23,37	
0,035	0,00021	1,98	3,96	7,92	0,025
0,01	0,000062	0,58	1,17	2,34	

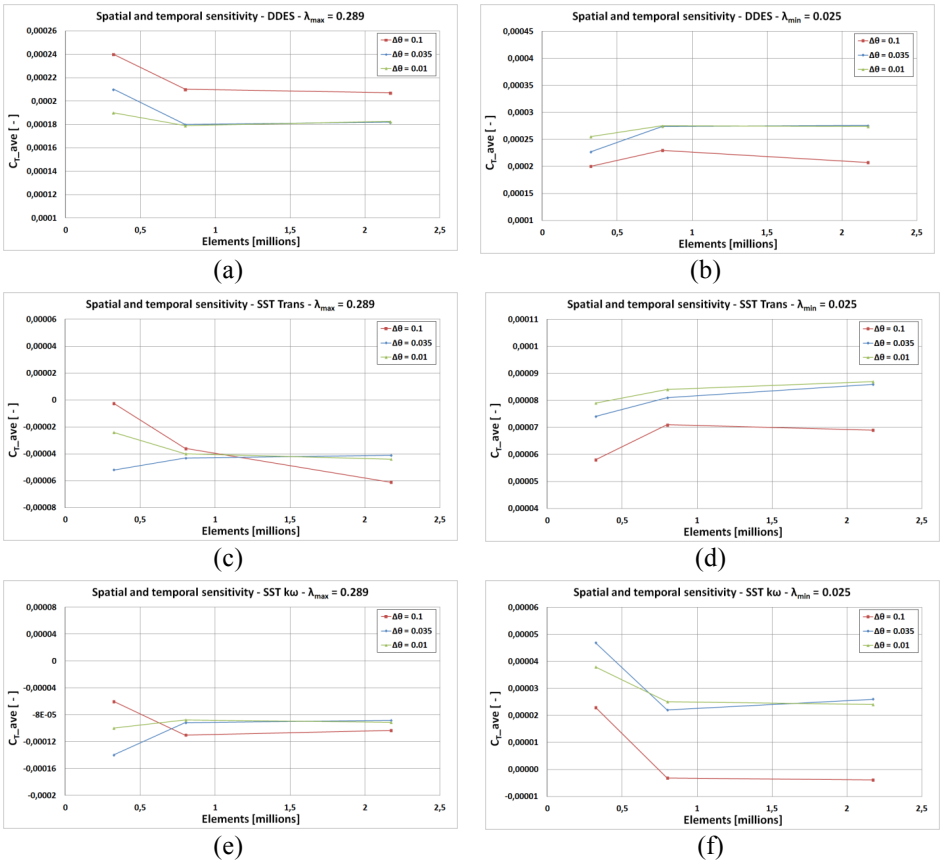

FIGURE 4. Average torque coefficient sensitivity analysis at λ_{max} and λ_{min} for different turbulence models

The main CFD solver settings are summarized in Table 4. The ANSYS Fluent transient solver was used with a coupled pressure-velocity coupling algorithm. The only thing to note was the use of optimized local correlation parameters for the SST transition formulation both in URANS and in DDES. This optimization was carried out by following what is reported in a previous work by the authors [23]. The number of iterations within each time step

was chosen in such a way to ensure that all the sub-iteration residuals were widely below 10^{-4}. The turbulence boundary conditions were set according to wind tunnel data and literature suggestions [12, 21]. The criterion used for the convergence evaluation was to have an average torque coefficient variation lower than 0.1% between two consecutive revolutions. This usually taken from three to five complete rotor revolutions. Once reached the convergence, the data were sampled for two subsequent revolutions. The five simulated operating conditions are shown in Table 4. The simulations were carried out on a HP Z820 workstation with 24 available threads for parallel calculation and 128 GB of RAM memory, using the GPU computation as well. The calculation time per revolution was approximately 58 hours with the SST k-ω model, 65 hours with the Transition SST model and 71 hours with the DDES model.

TABLE 4. Main CFD solver settings

Solver	ANSYS Fluent - Transient - Coupled		
Turbulence models	URANS Transition SST URANS SST k-ω Delayed DES with Transition SST		
Numerical schemes	Least squares cell based for gradients Second order upwind for all the equations Bounded central differencing for momentum in DDES Second order implicit for time differencing in URANS Bounded second order implicit for time differencing in DDES		
Rotation model	Sliding Mesh Model		
Iterations per time step	60		
Turbulence boundary conditions	Inlet: TI = 0.1%, TVR = 10 Outlet: TI = 5%, TVR = 10		
Convergence criterion	Average torque coefficient variation lower than 0.1% between two subsequent revolutions		
Simulated operating conditions	V_w = 11.1 m/s	n = 27 r/min	λ = 0.025
	V_w = 15.2 m/s	n = 133 r/min	λ = 0.092
	V_w = 17 m/s	n = 227 r/min	λ = 0.14
	V_w = 19.1 m/s	n = 362 r/min	λ = 0.198
	V_w = 21 m/s	n = 580 r/min	λ = 0.29

MODEL VALIDATION AND ANALYSIS OF THE RESULTS

The results of the experimental tests confirmed the fact that very small VAWT rotors, such that studied in the present work, were not able to produce high power compared to HAWTs of similar dimensions. As far as the experimental validation of the CFD model is concerned, in Fig. 5 the comparison between the measured and the calculated power coefficients is shown. As previously mentioned, the experiments were carried out using a mechanical braking system. In Fig. 5 the experimental data refers to three different constant braking loads equal to 25 g, 50 g and 75 g in mass. Due to the low torque produced by the rotor, the torque dissipated by the bearings limited the range of measurement approximately at $\lambda = 0.3$. Only the CFD DDES simulation results are reported in Fig. 5 because of the unphysical prediction obtained with the other turbulence models. As a matter of fact, both the URANS SST transition and SST k-ω model predicted negative power coefficients for almost the entire operating range of the rotor. Furthermore, in Fig. 5, Qblade Double Multiple Stream-Tube Model (DMSTM) simulation results are plotted. Qblade is an open source 1D code [24] which must be initialized using suitable polars for the airfoils. In this case, the experimental data of the NACA 0012 were taken from the literature [25], for an average cord Reynolds number of approximately 40,000. The DMSTM implemented within Qblade uses advanced models and corrections for tip losses, dynamic stall and virtual camber, similar to those used in the BEM theory for HAWTs [26]. The excellent accuracy of the CFD 2D model based on DDES is evidenced by the close proximity between experimental measurements and simulation results. This is a noticeable result considering the failure of the other turbulence models. However, in light of the extreme simplicity and rapidness of the Qblade model, the 1D results appear to be very surprising in terms of power coefficient prediction accuracy. Certainly, this result deserves further investigations in order to verify whether it is a mere chance or a generalizable result.

Some post-processing images are reported below. In Fig. 6 the contours of velocity magnitude for the three turbulence models tested demonstrate the strong differences in the flow-field prediction. The DDES results (Fig. 6 (a)) show structures which are smaller and more defined than those obtained from the RANS simulations. Both the RANS models seem to smooth the swirling structures more than the DDES model. Furthermore the flow separation

dynamic of the blades at azimuthal positions θ = 90° and 270° is very different, also between the transition and the SST k-ω models. In light of the validation obtained with the DDES model, the above would suggest that the RANS models over-estimate the dimensions of the flow structures and therefore the negative effects of the unsteady phenomena like dynamic stall and blade-vortex interaction in the down-wind sector.

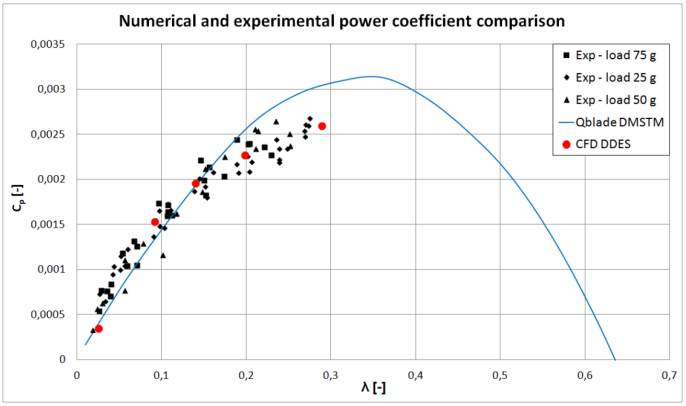

FIGURE 5. Comparison between numerical and experimental power coefficient

The above considerations appear to be confirmed in Fig. 7. Here, the contours of turbulent intensity for the three turbulence models are shown. The fact that the RANS models predict a massive and smooth turbulence production is highly evident. The DDES model instead predict much lower turbulence in smaller and more defined structures. Given the high accuracy in the power prediction, the DDES model appear to be more physically consistent to the real flow-field. Furthermore, the DDES results provide an explanation for the poor efficiency of such micro VAWTs as well. Indeed, Fig. 6 (a) and Fig. 7 (a) highlight the high stalled rotor conditions, emphasized by the very low Reynolds numbers. These are thus the main responsible factors for the low efficiency of this micro rotor.

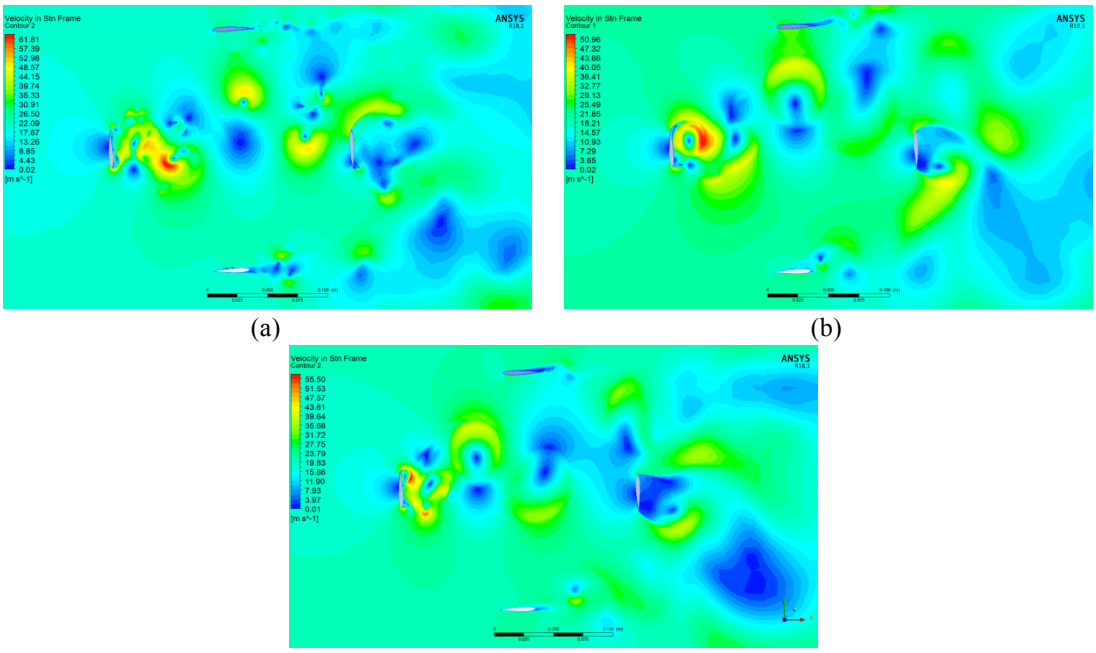

FIGURE 6. Contours of velocity magnitude for DDES (a), RANS Transition (b) and RANS SST k-ω (c) at 0° azimuthal position

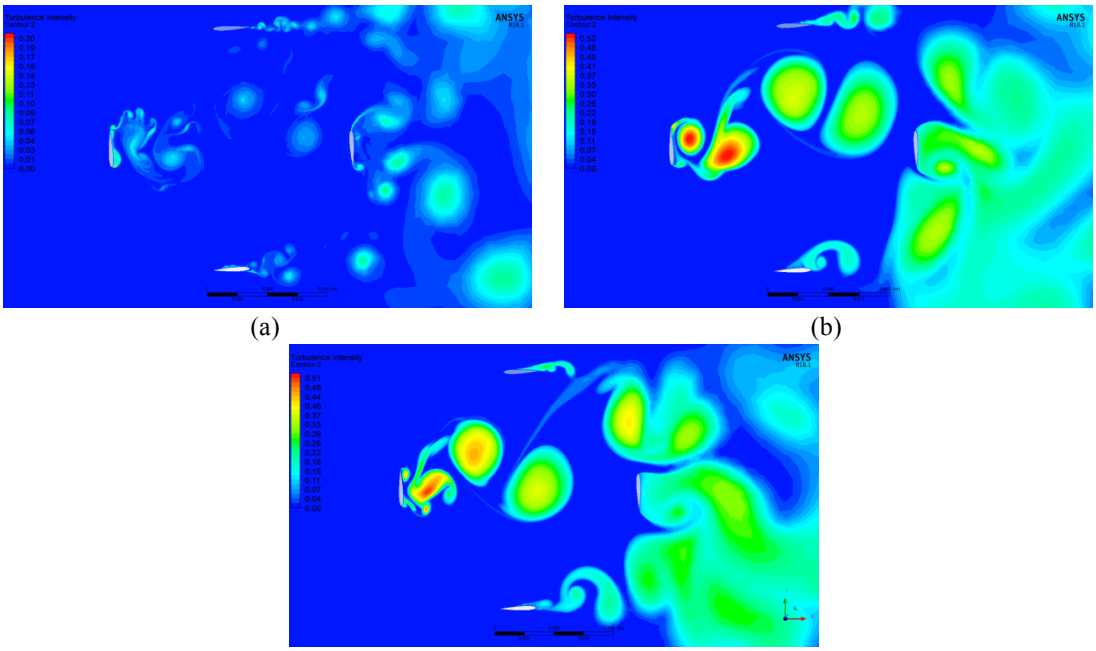

(a) (b)

(c)

FIGURE 7. Contours of turbulent intensity for DDES (a), RANS Transition (b) and RANS SST k-ω (c) at 0° azimuthal position

CONCLUSIONS

In the present paper the authors present the results of the implementation of a 2D CFD model for the simulation of a micro VAWT. The highly unstable conditions, related to the rotor operation, required a specific temporal and spatial discretization sensitivity study and a thorough evaluation of the turbulence models suitability. A very fine spatial and temporal discretization was necessary in order to capture the high vorticity gradients caused by the low tip speed operating range of such micro rotor. The study demonstrated that, due to the unstable conditions, an advanced Delayed Detached Eddie Simulation, coupled to a transition formulation for the RANS region, was the only one able to provide accurate results. Nevertheless the very fine grid and time step resolution, the RANS SST Transition model and SST k-ω model both led to unphysical torque predictions. The DDES model instead showed accurate power coefficient prediction compared to the experimental measurements. The post-processing analysis demonstrated that the RANS models massively overestimated the turbulence production therefore emphasizing too much the negative effects of dynamic stall and downwind blade-vortex interaction. Instead, the accuracy of the DDES simulations allowed for the identification of the causes of the poor efficiency of such micro VAWTs. The low Reynolds numbers and the small dimensions implied that the rotor is highly subjected to early flow separation and as a consequence, high negative dynamic stall effects. The availability of an accurate CFD model will allow the authors to identify an optimization strategy for these rotors in order to increase their efficiency. Use of suitable airfoils, specific pitch angles, vortex generators are just some of the simplest and cheapest techniques, whose effectiveness can be evaluated thanks to the CFD model developed in this work.

ACKNOWLEDGMENTS

This work has been financed by the University of Catania within the project “Piano della Ricerca Dipartimentale 2016-2018” of the Department of Civil Engineering and Architecture.

REFERENCES

1. F. J. Xu, F-G Yuan, L. Liu, J. Z. Hu, Y. P. Qiu, *Performance Prediction and Demonstration of a Miniature Horizontal Axis Wind Turbine* J. Energy Eng., 2013, 139(3): 143-152, DOI: 10.1061/(ASCE)EY.1943-7897.0000125

2. R. A. Kishore, T. Coudron, S. Priya *Small-scale wind energy portable wind turbine (SWEPT)* J. Wind Eng. Ind. Aerodyn. 116 (2013) 21–31 http://dx.doi.org/10.1016/j.jweia.2013.01.010
3. R. A. Kishore, S. Priya *Design and eperimental verification of a high efficiencysmall wind energy portable turbine (SWEPT)* J. Wind Eng. Ind. Aerodyn. 118 (2013) 12–19 http://dx.doi.org/10.1016/j.jweia.2013.04.009
4. M. Y. Zakaria, D. A. Pereira, M. R. Hajj *Experimental investigation and performance modeling of centimeter-scale micro-wind turbine energy harvesters* J. Wind Eng. Ind. Aerodyn. 147 (2015) 58–65 http://dx.doi.org/10.1016/j.jweia.2015.09.009
5. F. J. Xu, F. G. Yuan, J. Z. Hu, Y. P. Qiu *Miniature horizontal axis wind turbine system for multipurpose application* Energy 75 (2014) 216-224 http://dx.doi.org/10.1016/j.energy.2014.07.046
6. M. Bastankhah and F. Porté-Agel *A New Miniature Wind Turbine for Wind Tunnel Experiments. Part I: Design and Performance* Energies 2017, 10, 908; doi:10.3390/en10070908
7. R. Lanzafame, S. Mauro, M. Messina *Numerical and experimental analysis of micro HAWTs designed for wind tunnel applications* Int J Energy Environ Eng (2016) 7: 199. https://doi.org/10.1007/s40095-016-0202-8
8. Y. Mutlu, M. Çakan *Evaluation of in-pipe turbine performance for turbo solenoid valve system* Engineering Applications of Computational Fluid Mechanics (2018), 12:1, 625-634 DOI: 10.1080/19942060.2018.1506364
9. F. Balduzzi, A. Bianchini, R. Maleci, G. Ferrera, L. Ferrari *Critical issues in the CFD simulation of Darrieus wind turbines* Renewable Energy 85 (2016) 419-435 http://dx.doi.org/10.1016/j.renene.2015.06.048
10. F. Balduzzi, A. Bianchini, G. Ferrara, L. Ferrari *Dimensionless numbers for the assessment of the mesh and timestep requirements in CFD simulations of Darrieus wind turbines* Energy 97 (2016) 246-261 http://dx.doi.org/10.1016/j.energy.2015.12.111
11. A. Bianchini, F. Balduzzi, P. Bachant, G. Ferrara, L. Ferrari *Effectiveness of two-dimensional CFD simulations for Darrius VAWTs: a combined numerical and experimental assessment* Energy Conversion and Management 136 (2017) 318–328 http://dx.doi.org/10.1016/j.enconman.2017.01.026
12. Lanzafame, R., Mauro, S., Messina, M. *2D CFD modeling of H-Darrieus wind turbines using a transition turbulence model* Energy Proc Elsevier 45, pp. 131–140 (2014). Doi:10.1016/j.egypro.2014.01.015
13. B. Mannion, S. B. Leen, S. Nash *A two and three-dimensional CFD investigation into performance prediction and wake characterization of a vertical axis turbine* J. Renewable Sustainable Energy 10, 034503 (2018) DOI: 10.1063/1.5017827
14. H. Lei, D. Zhou, Y. Bao, Y. Li, Z. Han *Three-dimensional Improved Delayed Detached Eddy Simulation of a two-bladed vertical axis wind turbine* Energy Conversion and Management 133 (2017) 235–248 http://dx.doi.org/10.1016/j.enconman.2016.11.067
15. J. Thé, H. Yu *A critical review on the simulations of wind turbine aerodynamics focusing on hybrid RANS-LES methods* Energy 138 (2017) 257-289 http://dx.doi.org/10.1016/j.energy.2017.07.028
16. C.J. Simão Ferreira, H. Bijl, G. van Bussel, G. van Kuik *Simulating Dynamic Stall in a 2D VAWT: Modeling strategy, verification and validation with Particle Image Velocimetry data* Journal of Physics: Conference Series 75 (2007) 012023 doi:10.1088/1742-6596/75/1/012023
17. C. J. Simão Ferreira, A. van Zuijlen, H. Bijl, G. van Bussel and G. van Kuik *Simulating dynamic stall in a two-dimensional vertical-axis wind turbine: verification and validation with particle image velocimetry data* Wind Energ. 2010; 13: 1–17 DOI: 10.1002/we.330
18. Menter, F.R., Langtry, R., Volker, S. *Transition modeling for general purpose CFD codes* Flow Turb. Combust. 77, 277–303 (2006). doi:10.1007/s10494-006-9047-1
19. Langtry, R.B., Menter, F.R., Likki, S.R., Suzen, Y.B., Huang, P.G., Volker, S. *A correlation-based transition model using local variables—part I: model formulation* In: Vienna, ASME Paper No. ASME-GT-2004-53452; 2006
20. Langtry, R.B., Menter, F.R., Likki, S.R., Suzen, Y.B., Huang, P.G., Volker, S. *A correlation-based transition model using local variables—part II: test cases and industrial applications* ASME. J. Turbomach. 128(3), pp. 423–434 (2006)
21. Brusca, S., Lanzafame, R., Messina, M. *Low speed wind tunnel: design and build. In: Pereira, J.D. (ed.) Wind Tunnels: Aerodynamics, Models and Experiments*, chap 7, pp. 189–220. Nova Science Publishers, Inc., Hauppauge, NY. ISBN: 978-1-61209-204-1 (2011)
22. Spalart, P.R. *Young-Person's Guide to Detached-Eddy Simulation Grids* NASA/CR-2001-211032; NASA Langley Research Center: Hampton, VA, USA, 2001
23. S. Mauro, R. Lanzafame, M. Messina, D. Pirrello *Transition turbulence model calibration for wind turbine airfoil characterization through the use of a Micro-Genetic Algorithm* Int J Energy Environ Eng (2017) 8 pp.359–374 https://doi.org/10.1007/s40095-017-0248-2
24. D. Marten, J. Wendler, G. Pechlivanoglou, C. N. Nayeri, C. O. Paschereit *Qblade: an open source tool for design and simulation of horizontal and vertical axis wind turbines* International Journal of Emerging Technology and Advanced Engineering Volume 3, Special Issue 3: ICERTSD 2013, Feb 2013, pages 264-269 ISSN 2250-2459
25. Shedahl, R. E., Klimas, P. C. *Aerodynamic characteristics of seven symmetrical airfoil sections through 180-degree angle of attack for use in aerodynamic analysis of vertical axis wind turbines* 1981 Technical Report No. SAND80-2114, Sandia National Laboratories, Albuquerque, New Mexico
26. Lanzafame R. Mauro S. Messina M. *HAWT design and performance evaluation: Improving the BEM therory mathematical models* Energy Procedia Volume 82, 2015, pages 172-179 DOI: 10.1016/j.egypro.2015.12.015